Fabrication of a biocathode for formic acid production upon the immobilization of formate dehydrogenase from Candida boidinii on a nanoporous carbon

Naiara Hernández-Ibáñez, Alicia Gomis-Berenguer, Vicente Montiel, Conchi Maria Concepcion Ovin Ania, Jesús Iniesta

Chemosphere 291 (2022) 133117

Contents lists available at ScienceDirect

Chemosphere

journal homepage: www.elsevier.com/locate/chemosphere

Fabrication of a biocathode for formic acid production upon the immobilization of formate dehydrogenase from *Candida boidinii* on a nanoporous carbon

Naiara Hernández-Ibáñez [a], Alicia Gomis-Berenguer [b], Vicente Montiel [a], Conchi O. Ania [b,**], Jesús Iniesta [a,*]

[a] Physical Chemistry Department and Institute of Electrochemistry, University of Alicante, 03080, Alicante, Spain
[b] CEMHTI (UPR 3079, CNRS), University of Orléans, 45071, Orléans, France

HIGHLIGHTS

- High stability of enzyme CbFDH immobilized on a nanoporous carbon.
- Co-immobilization of CbFDH and Rh complex mediator on a nanoporous carbon.
- Fabrication of a biocathode for formic acid production at high scale.
- Formic acid production rate comparable to values reported in the literature.

GRAPHICAL ABSTRACT

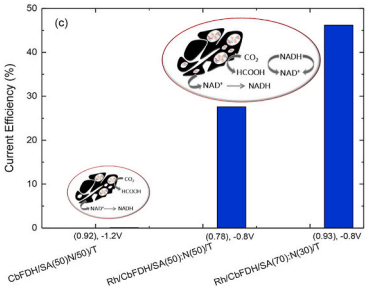

ARTICLE INFO

Handling Editor: Dr. E. Brillas

Keywords:
Formate dehydrogenase from *Candida boidinii*
Formic acid, NADH-regeneration
Mesoporous carbon
Biocathode

ABSTRACT

The immobilization of the non-metallic enzyme formate dehydrogenase from *Candida boidinii* (CbFDH) into a nanoporous carbon with appropriate pore structure was explored for the bioelectrochemical conversion of CO_2 to formic acid (FA). Higher FA production rates were obtained upon immobilization of CbFDH compared to the performance of the enzyme in solution, despite the lower nominal CbFDH to NADH (β-nicotinamide adenine dinucleotide reduced) cofactor ratio and the lower amount of enzyme immobilized. The co-immobilization of the enzyme and a rhodium complex as mediator in the nanoporous carbon allowed the electrochemical regeneration of the cofactor. Preparative electrosynthesis of FA carried out on biocathodes of relatively large dimensions (ca. 3 cm × 2 cm) confirmed the higher production rate of FA for the immobilized enzyme. Furthermore, the incorporation of a Nafion binder in the biocathodes did not modify the immobilization extent of the CbFDH in the carbon support. Coulombic efficiencies close to 46% were obtained for the electrosynthesis carried out at −0.8 V for the biocathodes prepared using the lowest Nafion binder content and the co-immobilized enzyme and rhodium redox mediator. Although these values may yet be improved, they confirm the feasibility of these biocathodes in larger scales (6 cm^2) beyond most common electrode dimensions reported in the literature (ca. a few mm^2).

* Corresponding author.
** Corresponding author.
E-mail addresses: conchi.ania@cnrs-orleans.fr (C.O. Ania), jesus.iniesta@ua.es (J. Iniesta).

https://doi.org/10.1016/j.chemosphere.2021.133117
Received 18 October 2021; Received in revised form 25 November 2021; Accepted 27 November 2021
Available online 30 November 2021

1. Introduction

CO_2 utilization through electrochemical reduction techniques for the production of chemical feedstocks such as formic acid (FA) (Del Castillo et al., 2015), formaldehyde (Nakata et al., 2014), methane (Marinoiu et al., 2017), methanol (Addo et al., 2011), ethanol (Yuan et al., 2018) or syngas (Hernández et al., 2017) represents an interesting strategy among currently investigated processes for CO_2 conversion. However, since CO_2 is a thermodynamically stable molecule, its electrochemical reduction is strongly limited by the kinetic barriers associated to the need to lower overpotentials, to activate CO_2 species, to increase the coulombic efficiencies and to enhance the selectivity of the products (Appel et al., 2013; Finn et al., 2012). In this context, numerous investigations have explored the use of metallic and non-metallic electrocatalysts and their composites for the conversion of CO_2 to fuels or feedstocks (e.g. Sn (Del Castillo et al., 2015), Au (Zhao et al., 2018), Cu (Li et al., 2016), Bi (Zhang et al., 2016a), graphene oxide, carbon nanotubes (Zhu et al., 2016), g-C_3N_4/carbon nanotube (Lu et al., 2016) to cite a few examples). Such electrocatalytic processes still face problems related to the long-term stability and low selectivity of the catalysts, and hence the economic viability of the process is strongly dependent on the electricity cost (Liu et al., 2016).

Alternatively, the use of enzymes as biocatalysts allows a better-controlled CO_2 reduction due to their high selectivity, leading to the formation of a specific fuel while avoiding side reactions. Several enzymes and microorganisms have been explored for the CO_2 reduction: *viz*. remodelled nitrogenase for the reduction of CO_2 to methane (Yang et al., 2012); non-metal formate dehydrogenases (FDH) or metal dependent (tungsten or molybdenum)-containing formate dehydrogenase (mFDH) for the reversible conversion of CO_2 and formic acid (Bassegoda et al., 2014); methylobacteries for the production of FA (Hwang et al., 2015); and dehydrogenases in consecutive electrochemical reduction reactions to simultaneously generate formaldehyde and methanol (Lanjekar and Gharat, 2011). Note in this regard that FA is an effective energy storage fuel (Rees and Compton, 2011), with a lower toxicity than methanol (Yu and Pickup, 2008), and that some FDH enzymes are able to catalyze the reversible interconversion of CO_2 to FA (Alissandratos et al., 2013; Lu et al., 2006; Hartmann and Leimkühler, 2013; Jollie and Lipscomb, 1991; Schirwitz et al., 2007; Amao, 2018). However, FDH enzymes generally require the cofactor β-nicotinamide adenine dinucleotide reduced (NADH) to achieve the reduction of CO_2 yielding FA according to reaction (1):

$$CO_2 + NADH \leftrightarrow^{CbFDH} HCOO^- + NAD^+ \quad (1)$$

The high price of NAD(H) cofactors prevents their stoichiometric use, for which their regeneration is needed to boost this reaction in practical applications. The electrochemical regeneration of NADH is generally carried out according to the following mechanisms (Ali et al., 2014):

$$NAD^+ + e^- \rightarrow \mathrm{NAD}^\bullet \quad (2)$$

$$NAD^\bullet + e^- + H^+ \rightarrow NADH \quad (3)$$

$$NAD^\bullet + NAD^\bullet \rightarrow NAD_2 \quad (4)$$

However, the slow kinetics of reaction (3) competes with the dimerization of $NAD^\bullet$ species in reaction (4), resulting in a loss of ca. 40% of cofactor in each regeneration cycle (Wu et al., 2013; Weckbecker et al., 2010). Therefore, the electrochemical regeneration has to be promoted by an indirect or mediated pathway, using redox mediators as hydride-transfer agents. Various redox mediators have been investigated for the indirect electrochemical regeneration of NADH, such as methylviologen (Hwang et al., 2015; Weckbecker et al., 2010; Sakai et al., 2016a), rhodium and iridium-based metal complexes (Tan et al., 2015; Sivanesan and Yoon, 2013), osmium polymers (Cui et al., 2007), or 9, 10-phenanthrenequinone (Sakai et al., 2017b). In this context, a paradigm for electrochemical regeneration of NADH refers to the use of (2,2′-bipyridyl) (Pentamethylcyclopentadienyl)rhodium complex, [Cp*Rh (bpy)Cl]Cl, that is able to bring down the potential for NADH regeneration at −0.8 V (Fig. ESI-1) (Hollmann et al., 2002; Walcarius et al., 2011; Steckhan et al., 1991).

On the other hand, the use of enzymes in electrochemical applications still has several challenges to face, mainly related to their cost and stability under variable reaction conditions -e.g., pH, temperature or ionic strength-, and to a proper electron transfer (ET) communication between the redox-active center of the biomolecule and the electrode surface. Immobilization strategies seem to be quite successful methods to overcome these challenges (Chapman et al., 2018). In the particular case of FDH from *Candida boidinii* (CbFdH), several studies have been reported on its immobilization/encapsulation on various substrates (e.g., glutaraldehyde, epoxy, amino-epoxy, glyoxyl or aminated substrates (Bolivar et al., 2007), modified magnetic nanoparticles (Demir et al., 2011), alginate-silicate hybrid gel, calcium alginate, polyvinyl alcohol or montmorillonite K (Lu et al., 2006), porous glass plate (Noji et al., 2017), metal organic frameworks (Rouf et al., 2021) or mesoporous carbons (Hernández-Ibáñez et al., 2021) for exploring its biocatalytic activity.

The bioelectrochemical reduction of CO_2 has been reported for FDH enzymes immobilized in various supports -e.g., carbon felt modified with alginate-silicate hybrid gel (Schlager et al., 2016), polystyrene nanofibers (Barin et al., 2019), nanoporous carbon black (Sakai et al., 2016a, 2016b; Sakai et al., 2017b), gold nanoparticles embedded on carbon black (Sakai et al., 2017a), pyrolytic graphite (Cordas et al., 2019), titanium dioxide (Sokol et al., 2018)-. Even though the feasibility of the bioelectrochemical CO_2 reduction has been demonstrated either for FDH in solution or encapsulated/adsorbed on appropriate substrates, the fabrication and deployment of biocathodes at high scale in bioelectrochemical reactors is still far for being a competitive technology compared to metal electrocatalysts-based processes.

In this study, we focus on the performance of the electrochemical reduction of CO_2 to FA using a biocathode constituted by the co-confinement of CbFDH and the complex [Cp*Rh (bpy)Cl]Cl, on a highly nanoporous carbon; the co-immobilization of the rhodium complex allows the regeneration of the NADH cofactor. A metal independent CbFDH was selected for this study due to its attractiveness in terms of low cost, commercial availability, mass produced and robustness. On the other hand, the use of NADH in solution as cofactor is simple in terms of mechanism reaction and moderate high yield (Kanth et al., 2013), while the use of the rhodium complex will regenerate the cofactor at relatively low overpotentials. The merit of this work points firstly at the fabrication of biocathodes with relatively large projected area (i.e., 2 cm × 3 cm), higher than those commonly reported in the literature for others FDH enzymes (i.e., a few mm^2). We have used a commercial mesoporous carbon for the immobilization of the enzyme and rhodium complex redox mediator, and explored the performance of the biocathode as a function of adsorbed protein, loading coverage and binder content for further utilization in a polymer electrolyte membrane electrochemical reactor (PEMER) (Diaz-Sainz et al., 2020). To evaluate the bioelectrochemical reduction of CO_2 to FA, preparative electrolyses were performed at different electrode potentials in the absence and presence of NADH cofactor and of redox mediator. Data have confirmed the beneficial effect of the co-confinement of the redox mediator and the enzyme CbFDH for the performance of the biocathodes, in terms of FA production and coulombic efficiencies compared to other bioelectrochemical systems (BES) based on the immobilization of FDH enzymes. This work also demonstrates the feasibility of the application of large dimensions biocathodes based on immobilized FDH enzymes for the bioelectrochemical reduction of CO_2 to FA.

2. Experimental

2.1. Chemicals and reagents

The non-metal dependent Formate dehydrogenase from *Candida boidinii* (lyophilized powder with ca. 5.0–15.0 units/mg protein), β-Nicotinamide adenine dinucleotide sodium salt (NAD^+, purity ≥97%), β-Nicotinamide adenine dinucleotide reduced dipotassium salt (NADH, purity ≥97%), Nafion perfluorinated resin (5 wt% isopropyl alcohol/water solution), pentamethylcyclopentadienylrhodium (III) chloride dimer (purity 97%) and 2,2′- bipyridyl (purity ≥99%) were purchased from Sigma Aldrich. The rest of chemicals were of the highest purity available. The redox mediator [Cp*Rh (bpy)Cl]Cl (2,2′-bipyridyl) (pentamethylcyclopentadienyl)rhodium) used in the regeneration of NADH was synthetized by following the procedure as described elsewhere (Hollmann et al., 2002; Walcarius et al., 2011). The selected nanoporous carbon is a commercially available carbon material commercialized by Ingevity (formerly Westvaco) under the name of Nuchar® SA-30. It is a biomass-derived carbon obtained upon chemical activation with phosphoric acid. The carbon was chosen based on its porosity, chemical composition and availability for large-scale applications. All solutions were prepared using doubly distilled water with a resistivity not less than 18.2 MΩ cm. Unless otherwise stated, enzyme solutions were freshly prepared either in 0.010 M or 0.10 M sodium phosphate buffer solution (NaPB) at pH 7.4 using Na_2HPO_4, NaH_2PO_4 salts (from Sigma-Aldrich) and stored at 4 °C.

2.2. Physicochemical and textural characterization

The porosity of the carbon was determined by N_2 adsorption/desorption isotherms at −196 °C recorded in a volumetric analyzer (Quantachrome Instruments). Before the analysis, the sample was degassed under dynamic vacuum at 250 °C for 8 h. SEM images and mapping analysis of the electrodes were recorded in a microscope HITACHI S–3000 N coupled with an energy dispersion X-ray microanalysis EDX system Quantax 400 from Bruker. X-ray photoelectronic spectroscopy (XPS) experiments were collected in a K-Alpha Thermo Scientific spectrometer using monochromatic AlKα (1486.6 eV) radiation at 3 mA × 12 kV. Spectra of dried samples were recorded using a 400 μm (microns) diameter analysis area. Processing of the XPS spectra was performed in Avantage software, with energy values referenced to the C 1s peak of adventitious carbon located at 284.6 eV, and a Shirley-type background. Thermogravimetric profiles were carried out in a Setaram Labsys thermobalance using ca. 10 mg of sample, under argon atmosphere (100 mL/min) and at a heating rate of 10 °C/min from 25 up to 900 °C. A complete physicochemical characterization of the porous carbon support in terms of N_2 adsorption/desorption isotherm, pore size distribution determination, particle size and surface chemistry is provided in the Electronic Supplementary Information Fig. (ESI-2 to ESI-5).

2.3. CbFDH and [Cp*Rh(bpy)Cl]Cl immobilization

CbFDH and [Cp*Rh (bpy)Cl]Cl solutions were prepared in 10 mM NaPB at pH 7.4 (initial concentrations of 0.5 and 1.0 mg mL^{-1} for CbFDH and [Cp*Rh (bpy)Cl]Cl, respectively). An adequate amount of the nanoporous carbon was added to either the enzymatic or the Rh complex solutions to reach a dispersion of ca. 1.0 mg mL^{-1}, and then stirred during 6 d at 4 °C under deaerated conditions. Thereafter, the carbon dispersions were centrifuged at 1300 rpm for 5 min, and the supernatant solution was discarded. The weakly adsorbed species were removed by rinsing the carbon several times with 10 mM NaPB at pH 7.4. The amounts of CbFDH and [Cp*Rh (bpy)Cl]Cl immobilized were calculated from the mass balance of the species remaining in solution and detected by UV–Vis spectrophotometry (ca. 280 and 356 nm for CbFDH and [Cp*Rh (bpy)Cl]Cl, respectively). After the immobilization and washing, the loaded carbon powders were redispersed in 1.0 mL 0.1 M NaPB at pH 7.4 and stored at 4 °C until further use. The nomenclature of the carbon dispersions is as follows: SA for the nanoporous carbon dispersed in NaPB; CbFDH/SA after the immobilization of CbFDH and Rh/SA after the immobilization of the Rh complex mediator.

For the preparation of the electrodes, the stored carbon dispersions -namely SA and Rh/SA-were sonicated for 15 min (Ultrasons P, Selecta); then an adequate volume of 5 wt% Nafion aqueous solution was added to the dispersion to reach a final concentration of ca. 20 wt% Nafion vs the weight of solid residue. The mixture was sonicated for 40 min at a temperature lower than 30 °C. Then ca. 20 μL of the carbon ink was drop-casted onto a glassy carbon electrode surface (GCE, 3.0 mm diameter, Goodfellow) and dried under nitrogen atmosphere. The GCE was previously polished using alumina powders (ca. 1.0, 0.3 and 0.05 μm) and water as lubricant. The nomenclature of the electrodes was Z/GCE, where Z stands for the composition of the ink (e.g., SA/GCE, Rh/SA/GCE).

2.4. CbFDH activity control

The catalytic activity of the enzyme was determined spectrophotometrically recording the absorbance increment of NADH production at 340 nm during the oxidation of formate to CO_2, as reported elsewhere (Bolivar et al., 2007). An activity value of 5.8 U per mg of CbFDH was obtained. After the immobilization on the nanoporous carbon, the activity of the enzyme was certified by monitoring the synthesis of FA. Briefly, 410 μL of 1.0 mM NADH in 0.1 M NaPB at pH 7.4 were added to 1.0 mL of CbFDH in solution (ca. 0.35 mg CbFDH/mL) or to a CbFDH/SA dispersion (ca. 1.0 mg CbFDH/SA) previously saturated with CO_2 by continuously bubbling with a CO_2 flow of ca. 100 mL/min. The chemical reaction was carried out for 5 h at 20 ± 2 °C. Then, the CbFDH/SA suspensions were centrifuged at 13,000 rpm for 5 min, and the supernatant was removed for quantifying the formation of FA. When the reaction was carried out using CbFDH in solution, the protein solution was filtered out using a 10 kDa centrifugal filter. FA concentration was determined using an ion chromatograph equipped with chemical suppression (Metrohm, 850 ProfIC Acuma MCS).

2.5. Preparation of the biocathodes

Initially, different carbon inks were prepared consisting of an alcoholic dispersion (isopropanol) of the nanoporous carbon SA (ca. 2 wt% solids) mixed with various amounts of Nafion (carbon to Nafion weight percentage ratios of 50/50 and 70/30 wt/wt. %) and sonicated for 45 min. Then, the carbon inks were sprayed onto a 3 cm × 3 cm Toray carbon paper substrate (TGPH-120) placed on a hot metallic plate kept at 90 °C to facilitate the evaporation of the solvent. The carbon ink flow was controlled during the spraying process to get a homogeneous surface by sight. After airbrushing, the film was weighted to determine the average loading coverage (Γ) in mg of carbon per cm^2 of projected area; values of Γ of 0.50, 0.78, 0.83 and 0.92 mg cm^{-2} were obtained. The nomenclature of the electrodes was SA(x):N(y)/T, where x and y stand for the amount of carbon and Nafion, respectively, and T refers to the Toray carbon paper substrate.

Due to the porous nature of the carbon, electrodes SA(x):N(y)/T were immersed in 0.1 M NaPB pH 7.4 overnight prior the immobilization of CbFDH and the mediator, in order to guarantee the wettability of the inner porosity. CbFDH immobilization was carried out by immersion of the electrodes SA(x):N(y)/T in a 30 mL saturated argon solution containing 0.125 mg CbFDH mL^{-1} in 10 mM NaPB at pH 7.4; the mixtures were stirred for 5 d at 4 °C. For the immobilization of the [Cp*Rh (bpy)Cl]Cl mediator, the biocathode loaded with the enzyme (e.g. CbFDH/SA (x):N(y)/T) was immersed in 30 mL of a 0.2 mg mL^{-1} [Cp*Rh (bpy)Cl]Cl solution in 10 mM NaPB pH 7.4, and stirred for 5 d at 4 °C. The resulting biocathode was labeled as Rh/CbFDH/SA(x):N(y)/T. The amounts of both CbFDH and Cp*Rh (bpy)Cl immobilized were calculated again from the mass balance of the species remaining in solution by UV–Vis

spectrophotometry (*vide supra*). All biocathodes were thoroughly rinsed with 10 mM NaPB pH 7.4 and stored at 4 °C immersed in the same buffer solution under deaerated conditions.

2.6. Electrochemical measurements

Electrochemical measurements were taken using a potentiostat/galvanostat system Autolab PGSTAT X (Eco Chemie, the Netherlands) controlled by Autolab GPES software version 4.9 for Windows XP. For the electrochemical characterization of the adsorbed mediator on the nanoporous carbon, experiments were performed in a three-electrode electrochemical cell using a gold wire as a counter electrode, AgCl/Ag (1.0 M KCl) as reference electrode, and Rh/SA/GCE as working electrode. Electrochemical measurements were taken at 20 ± 2 °C under deaerated conditions using an argon stream during the electrochemical experiment.

Preparative electrolyses for FA production were carried out in an H-shape two compartment electrochemical cell (Fig. ESI-6), using a cationic ion exchange membrane Nafion 112 (Dupont, France); each chamber was filled up with 65 mL with 0.1 M NaPB at pH 7.4. Experiments were performed under controlled potential using the Autolab potentiostat/galvanostat as reported above. The counter electrode was a boron doped diamond (BDD) sheet placed in the anodic compartment. Either Rh/CbFDH/SA(x):N(y)/T or CbFDH/SA(x):N(y)/T biocathodes acted as working electrodes in the cathodic compartment, whereas the reference electrode was a AgCl/Ag (3 M KCl) through a luggin located at the cathodic compartment. Unless it is stated, all potentials were referred to AgCl/Ag. Prior the electrochemical experiments, the biocathodes were conditioned in 0.1 M NaPB pH 7.4; also, the cathodic compartment was deoxygenated by bubbling an argon stream for 30 min and then saturated with CO_2, maintaining a constant flow rate of 150 mL/min through the solution during the whole electrolysis. About 4.5 mg of NADH were added to the cathodic solution before starting the electrolysis to reach a final concentration of ca. 0.10 mM. The cathodic solution was continuously stirred during the electrolysis. FA concentration was determined by ionic chromatography (*vide supra*), and the coulombic efficiency for FA production (Θ_{HCOOH}) was calculated as follows: $\Theta_{HCOOH} = \frac{n_{HCOOH} \times \frac{\vartheta_e}{\vartheta_p} \times F}{Q}$.where n_{HCOOH} is the amount of FA produced (mol), $\frac{\vartheta_e}{\vartheta_p}$ is the number of electrons per mol of FA (2 electrons per mol of FA), F is the Faraday's constant (96,485 C mol^{-1}) and Q is the circulated charge (C) during the electrolysis (Sánchez-Sánchez et al., 2003).

3. Results and discussion

3.1. Preparation and electrochemical characterization of the biocathodes

First of all, we have explored the immobilization feasibility of CbFDH on the selected nanoporous carbon (Fig. ESI-7A). The amount of enzyme immobilized in the carbons was ca. 0.375 mg CbFDH/mg carbon under the experimental conditions used, corresponding to a complete uptake from solution after 5 d of stirring. The uptake is in agreement with the textural features of the selected carbon evaluated from gas adsorption data (Fig. ESI-2, Table ESI-1), revealing the presence of mesopores wide enough to accommodate the rugby-like shaped CbFDH protein. Indeed, even though the exact dimensions of the enzyme are uncertain -as they depend on several factors such as the confinement state, nature of the surface, or humidity-, the estimated values for CbFDH according to literature are ca. a:b:c 5.35, 6.85, 10.95 nm per unit cell (Schirwitz et al., 2007). On the other hand, the selected nanoporous carbon has a relatively high surface area (ca. 1554 $m^2\ g^{-1}$) and an important contribution of mesopores (ca. 63% of overall porosity) (Fig. ESI-2B). This demonstrates that the pore size distribution of the carbon is effective for the immobilization of CbFDH, and contrasts with other studies reporting the immobilization of the enzyme in porous materials with wider pores of ca. 40–50 nm (Sakai et al., 2017b; Noji et al., 2017; Rouf et al., 2021). It also indicates that the dimensions of the enzyme commensurate the average mesopore size of the carbon, which is expected to favor the stability of the immobilized enzyme. Based on the dimensions of CdFDH (*vide supra*) only the fraction of pores above 5 nm would be accessible for the immobilization of the enzyme (ca. 44% of the overall porosity, Fig. ESI-2B), with optimal confinement in pores of dimensions between 5 and 15 nm (ca. 51% pore fraction). This is in agreement with our previous study where it was observed that the immobilization of CbFDH is controlled by the morphology of the pores, with carbons characterized by high mesopore volumes showing low CbFDH uptakes due to the poor accessibility of the enzyme to the body of the pores when these are connected via narrow necks (Hernández-Ibáñez et al., 2018, 2021).

The successful immobilization of the enzyme in the pores of the carbon was investigated following the catalytic activity of the confined enzyme for the reduction of CO_2 to FA in 0.1 M NaPB. Table 1 compiles the results about FA production compared to that obtained using CbFDH in NaPB solution ($CbFDH_{sol}$) with the same nominal amount of NADH as cofactor. For this, the amount of enzyme immobilized on carbon SA was ca. 0.32 mg CbFDH/mg carbon; therefore for a proper comparative study, the same amount of enzyme was used in solution. The concentration of NADH (0.5 mM) was selected at the highest concentration as possible in order to favor the shifting of the equilibrium to the formation of formate for the reaction as written in reaction (1). In this regard, it should be pointed out that concentrations over 0.4 mM NADH have been reported to be detrimental for the stability of the enzyme (Kim et al., 2014). Thus despite the neither the reaction in solution nor with the immobilized enzyme immobilization have been optimized, the nominal production of FA can be used as a fair comparison since they have been carried out in similar conditions (even if the reaction itself is sensitive to various variables such as the concentration of NADH, *vide supra*).

For the reaction carried out using $CbFDH_{sol}$, the production rate of FA was $3.0{\cdot}10^{-5}$ μmol $mg^{-1}_{FDH}{\cdot}min^{-1}$ for a NADH to CbFDH ratio (mol/mol) of 202. On the contrary, for the immobilized enzyme ($CbFDH_{im}$) with a similar NADH to CbFDH molar ratio (222), the nominal production of FA was two orders of magnitude higher than that of $CbFDH_{sol}$. This is most outstanding considering the low CbFDH to NADH ratio used, and it may be attributed to a: i) more stable conformation and stability of the enzyme in the nanoconfined state, as demonstrated in our earlier studies using a series of mesoporous carbons with different pore size distributions (Hernández-Ibáñez et al., 2021); and/or ii) to the high affinity of CO_2 molecules to be adsorbed on the pores of the carbon (Kaneko and Rodríguez-Reinoso, 2019), thereby favouring the interaction with the active centres of the enzyme and thus improving the reaction kinetics of FA with respect to CbFDH in solution. Such difference in the FA production rate between $CbFDH_{sol}$ and $CbFDH_{im}$ could also be ascribed to the effects of local pH gradients, local higher CO_2 concentration inside the pores or the effect of vigorous bubbling of CO_2, that could render a quick and partial inactivation of the enzyme in solution compared to $CbFDH_{im}$ (Bolivar et al., 2007). According to data compiled in Table 1, it is also worth noting that the amount of NADH used for the

Table 1
Comparative results for the biochemical reduction of CO_2 towards formic acid (FA) performed with enzyme CbFDH in solution ($CbFDH_{sol}$) and immobilized on nanoporous carbon SA ($CbFDH_{im}$) in 0.1 M NaPB pH 7.4 at 20 ± 2 °C under continuous CO_2 bubbling with a flow rate of 100 mL min^{-1}; reaction time is 5 h; reaction volume is 1.41 mL.

	CbFDH	$NADH_{sol}$	NADH/CbFDH ratio	FA production	
	mg	mg	mol/mol	μmol min^{-1}	μmol $mg^{-1}_{CbFDH}{\cdot}min^{-1}$
$CbFDH_{sol}$	0.35	0.58	202	$1.0{\cdot}10^{-6}$	$3.0{\cdot}10^{-5}$
$CbFDH_{im}$	0.32	0.58	222	$4.3{\cdot}10^{-4}$	$1.33{\cdot}10^{-3}$

formation of FA corresponds to ca. 20% of the starting concentration of NADH when using $CbFDH_{im}$, which is far from the theoretical value taking into account the forward reaction as written in reaction (1). Such a low value can be explained by formate reoxidation (reverse reaction as written in reaction (1)) which is thermodynamically more favoured, according to calculations exposed in (Jayathilake et al., 2019) and the concomitant adsorption of NADH on the nanoporous carbon (*vide infra*). The final pH of the buffer solution for experiments carried out with free and immobilized CbFDH (see Table 1) reached ca. 6.4, discarding therefore the degradation of NADH at low pH (Wu et al., 1986). Furthermore, it should be mentioned that neither formate adsorption on the carbon SA nor formate production were observed in the absence of the enzyme immobilized on the carbon support.

Lixiviation tests corroborated the long-term stability of the confined enzyme upon storage in the buffer solution for several months, with no enzyme leaching to the solution. The use of slight large pores with a narrowest pore sizes distribution for the immobilization of CbFDH has been also performed by the authors demonstrating again negligible leaching of the enzyme for a long period of storage at 4 °C. Hence, a commensurate confinement of CbFDH faces on unfolding, thereby increasing the stability and the catalytic activity under extreme and harsh conditions (Ren et al., 2020).

In the case of [Cp*Rh (bpy)Cl]Cl (Fig. ESI-7B), the amount of Rh complex retained on the carbon after 5 d was 0.38 mg/mg. The electrochemical behavior of the Rh redox immobilized on the nanoporous carbon (sample Rh/SA/GCE) in the absence and presence of the NAD^+ cofactor is shown in Fig. 1. On the first negative scan, a cathodic peak appeared at around −0.65 V corresponding to the electrochemical reduction of Rh(III) to Rh(I) species. On the reverse scan, an oxidation shoulder was observed at −0.3 V, with a lower current intensity compared to the cathodic one. The current of the cathodic peak increased proportionally with the scan rate (data not shown); this electrochemical pattern is in agreement with data reported in the literature about the redox behavior of [Cp*Rh (bpy)Cl]Cl in neutral or alkaline pH (Steckhan et al., 1991), and is attributed to the protonation of the Rh(I) complex to form a hydride complex. The electrochemical response of [Cp*Rh (bpy)Cl]Cl in solution using a glassy carbon electrode (Fig. 1, inset) shows a peak at −0.7 V on the first scan, similar to that recorded when the mediator is confined on the nanoporous carbon.

The performance of the redox mediator for the electrochemical regeneration of NADH was confirmed by the increase in the cathodic current peak at −0.72 V when the measurements were carried out in the presence of 1 mM NAD^+ (Fig. 1). This confirmed the fast reduction of NAD^+ to NADH involving the oxidation of Rh(I) to Rh(III) species, which are further electrochemically reduced to Rh(I) (Steckhan et al., 1991; Hernández-Ibáñez et al., 2018) (Fig. ESI-1). Similar behavior was observed for the immobilized Rh complex and in solution, and these results are in agreement with those reported by Minteer and coworkers (2015). The electrooxidation of NADH in the absence of the Rh complex took place around −1.2 V vs the reference electrode, which is far from that one occurring for the Rh complex electroreduction. Hence, it is expected that the preparative synthesis for the bioelectroreduction of CO_2 at −0.8 V would preclude the formation of inactive isomers of NADH or dimers (Rees and Compton, 2011) (*vide infra*).

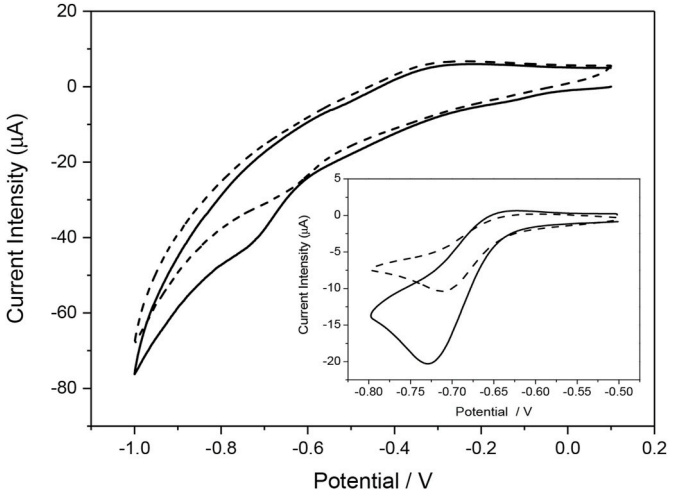

Fig. 1. Cyclic voltammetry responses of Rh/SA/GC electrode in the absence (dashed line) and presence (solid line) of 1.0 mM NAD^+ in 0.1 M NaPB pH 7.4. Scan rate: 5 mV s^{-1}. First scan recorded. Inset figure depicts the cyclic voltammetry responses of 1.0 mM [Cp*Rh (bpy)Cl]Cl complex in solution in the absence (dashed plot) and presence (solid line) of 0.5 mM NAD^+ using naked glassy carbon as working electrode. Scan rate 50 mV s^{-1}. First scan recorded.

Concerning the biocathodes, various electrodes SA(x):N(y)/T were prepared using two different carbon to Nafion ratios (50:50 and 70:30) so as to obtain an optimum mechanical cohesion of the biocathode film on the Toray carbon substrate. Fig. 2 depicts the SEM images of the SA (x):N(y)/T electrodes compared to the bare Toray paper used as substrate for various carbon loading coverages. All the samples displayed a uniform film covering the Toray substrate when a coverage of 0.5 mg cm^{-2} was achieved (Fig. 2a and c). Also, the amount of Nafion content present in the ink did not seem to affect the carbon loading coverage onto the Toray carbon substrate, nor the adherence or the cohesion of the films.

We next tackled the immobilization of the enzyme on the different SA(x):N(y)/T electrodes at various carbon loading coverages. Data in Fig. 3 reveal that for the same carbon loading (i.e., Γ of 0.5), the amount of immobilized CbFDH is higher when the amount of Nafion is the lowest, i.e., 30 wt%. It is worth pointing out that this is the minimum amount of Nafion that guarantees a proper cohesion of the films; in contrast, for Nafion concentrations higher than 50 wt%, the immobilization of CbFDH was compromised. Moreover, increasing the carbon loading coverage of the films resulted in higher CbFDH uptakes. For instance, 0.35 mg CbFDH/mg carbon were immobilized on electrode SA (70):N (30)/T with a loading coverage Γ of 0.92. This amount of enzyme immobilized per mg of carbon for the electrode built on Toray carbon paper is almost the same than that obtained upon immobilization on the nanoporous carbon dispersed in NaPB solution (0.375 mg CbFDH/mg carbon) as seen in Table 1 (*vide supra*). This finding confirms that the accessibility of the enzyme on the pores of the carbon support casted on the Toray carbon paper support is not hindered by the Nafion binder present in the carbon ink, thereby the scaling up fabrication of biocathodes of larger dimensions would seem feasible. Finally, the immobilization of the redox mediator was performed on biocathodes CbFDH/SA (70):N (30)/T and CbFDH/SA (50):N (50)/T, with carbon loading coverage values of 0.93 and 0.72, respectively. The [Cp*Rh (bpy)Cl]Cl loading was 0.35 mg/mg carbon film in both cases, which is interestingly in agreement with the value of 0.38 mg/mg obtained for the immobilization on the carbon dispersed in a NaPB solution. Thus, as in the case of the enzyme, it can be concluded that the immobilization is not affected by the carbon to Nafion ratio. Furthermore, the distribution of [Cp*Rh (bpy)Cl]Cl complex in the biocathodes surface was quite homogeneous, as seen in Fig. ESI-8; this suggests that the immobilization of the enzyme does not block the accessibility of the mediator [Cp*Rh (bpy)Cl]Cl to the porous network of the carbon (e.g., most likely the microporosity and the narrow mesoporosity).

3.2. Figures of merit for the production of FA in the prepared biocathodes

The bioelectrochemical reduction of CO_2 ($BERCO_2$) was carried out following two different approaches as depicted in Fig. 4. The first approach faces the reaction in the absence of a redox mediator (biocathode CbFDH/SA(x):N(y)/T), with the electrosynthesis potential set up at −1.2 V for the direct electrochemical regeneration of NADH (Ali et al., 2014; Azem et al., 2004) according to reactions (2)–(4). The

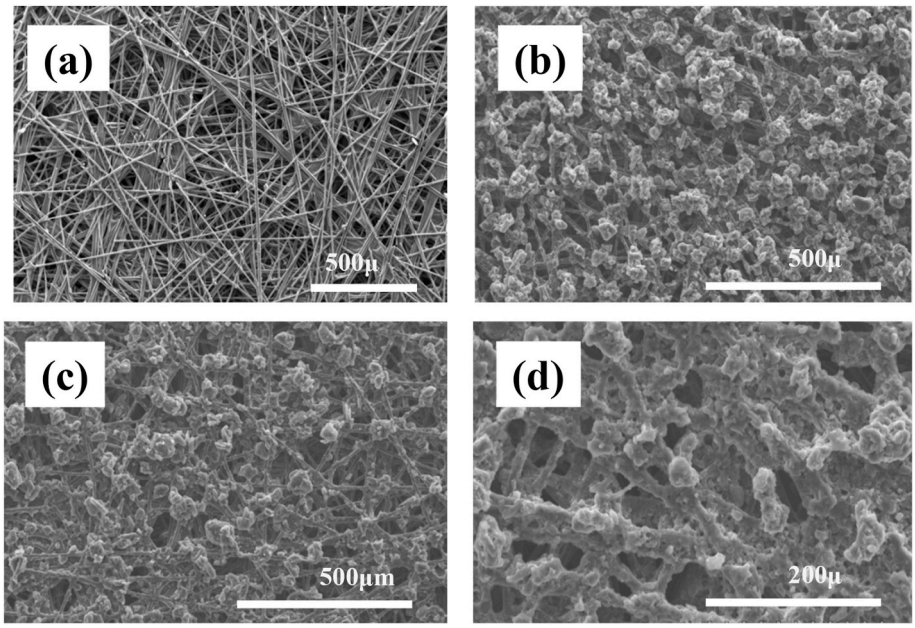

Fig. 2. SEM images of (a) Toray carbon paper used as underlying substrate; (b) SA (70):N (30)/T electrode with a coverage (Γ) of 0.5 mg cm^{-2}; (c) SA (50):N (50)/T electrode with Γ of 0.5 mg cm^{-2} and (d) SA (70):N (30)/T electrode with Γ of 0.92 mg cm^{-2}.

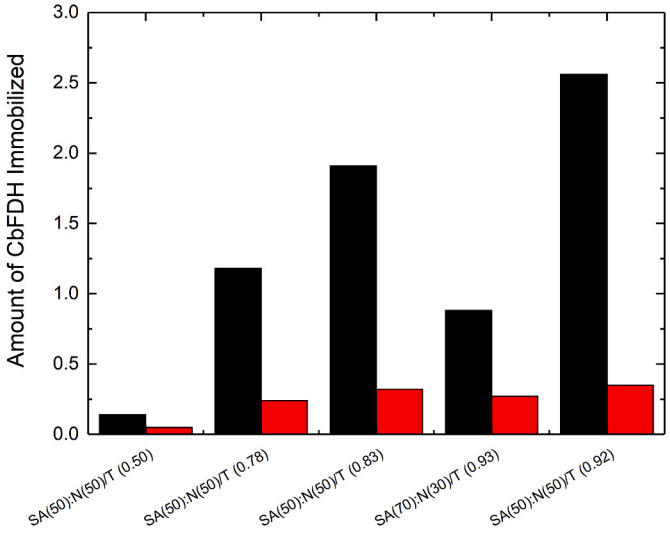

Fig. 3. CbFDH immobilization on carbon-based electrodes as a function of coverage (Γ) and carbon to Nafion ratios (wt.%). The amount adsorbed is expressed in terms of mg of CbFDH adsorbed (black bars), or mg CbFDH adsorbed per mg of carbon (red bars). The immobilization of CbFDH on the Toray carbon paper substrate was negligible.

second electrochemical approach is based on the use of biocathodes Rh/CbFDH/SA(x):N(y)/T (i.e., in the presence of a redox mediator co-immobilized in the porosity of the carbon), with the electrode potential set at −0.8 V, a more advantageous value for the regeneration of NADH (Sivanesan and Yoon, 2013; Hollmann et al., 2002). For comparative purposes, control electrosynthesis (absence of enzyme) were carried out on electrode SA (50):N (50)/T (Γ of 0.8) at the same electrode potentials (i.e., −1.2 and −0.8 V) during 5 h, in the absence and presence of NADH cofactor in solution.

Fig. 5 displays the FA concentration (in mg L^{-1}) and production (in µmol h^{-1} mg^{-1} of CbFDH) along with the current efficiencies of the most representative bioelectrosynthesis reactions carried out to explore the feasibility of both approaches considered. First of all, it should be mentioned that the control experiments for the electrochemical reduction of CO_2 on the carbon electrode (SA (50):N (50)/T) in the absence of the enzyme confirmed that the nanoporous carbon used as support is not an electroactive material for the production of FA. This is in agreement with other studies from the literature reporting negligible electrocatalytic activities for the reduction of CO_2 to CO, CH_4 or formate on metal-free carbons at potentials below −1 V (Li et al., 2016; Song et al., 2020; Hu et al., 2018; Karaman, 2021). Such negligible electrocatalytic activity of the studied nanoporous carbon alone is expected given its low surface functionalization (see Fig. ESI-4 and Fig. ESI-5), also in agreement with other authors (Yuan et al., 2018; Zou et al., 2017), The direct NADH electrochemical regeneration (i.e., without a redox mediator) was also explored on biocathode CbFDH/SA (70):N (30)/T (Γ of 0.5) at −1.2 V. Data confirmed a very low FA production rate (ca. 0.05 µmol h^{-1} $mg_{CbFDH}{}^{-1}$) and a low nominal FA concentration (ca. 0.32 mg L^{-1}) upon the direct electrochemical regeneration, as shown in Fig. 5; this is in agreement with the low current efficiencies reported in the literature for the electrochemical regeneration of NADH cofactor on various carbon electrodes (Ali et al., 2014; Moiroux and Elving, 1979).

In contrast, both biocathodes Rh/CbFDH/SA (50):N (50)/T and Rh/CbFDH/SA (70):N (30)/T at −0.8 V rendered FA concentrations of 2.4 and 13.3 mg L^{-1}, respectively. The higher FA concentration obtained for the latter biocathode can be attributed to the higher amount of protein immobilized (coverage is also higher). Nonetheless, in terms of FA production rates normalized per amount of the enzyme, the FA production of the biocathode Rh/CbFDH/SA (70):N (30)/T (Γ of 0.93) is still ca. twice higher than that of Rh/CbFDH/SA (50):N (50)/T (Γ of 0.78), also with a higher coulombic efficiency (near ca. 46%), as seen in Fig. 5.

This performance is in line with those reported in the literature for the $BERCO_2$ using CbFDH. In this regard, it should be emphasized that, most works on the electrosynthetic reduction of CO_2 with NAD-dependent FDH enzyme have been performed in solution, with scarce works on the immobilized enzyme and none of them (to the best of our knowledge) on porous carbons. For instance, Kim et al. (2014) reported a FA production of 2.1 10^{-3} µmol min^{-1} mg^{-1} after 5 h of reaction using a copper foil cathode and [Cp*Rh (bpy)Cl]Cl as mediator, slightly lower than herein reported values for biocathode Rh/CbFDH/SA (70)/N (30)/T (25·10^{-3} µmol min^{-1} mg^{-1} CbFDH) (Fig. 5); this corroborates

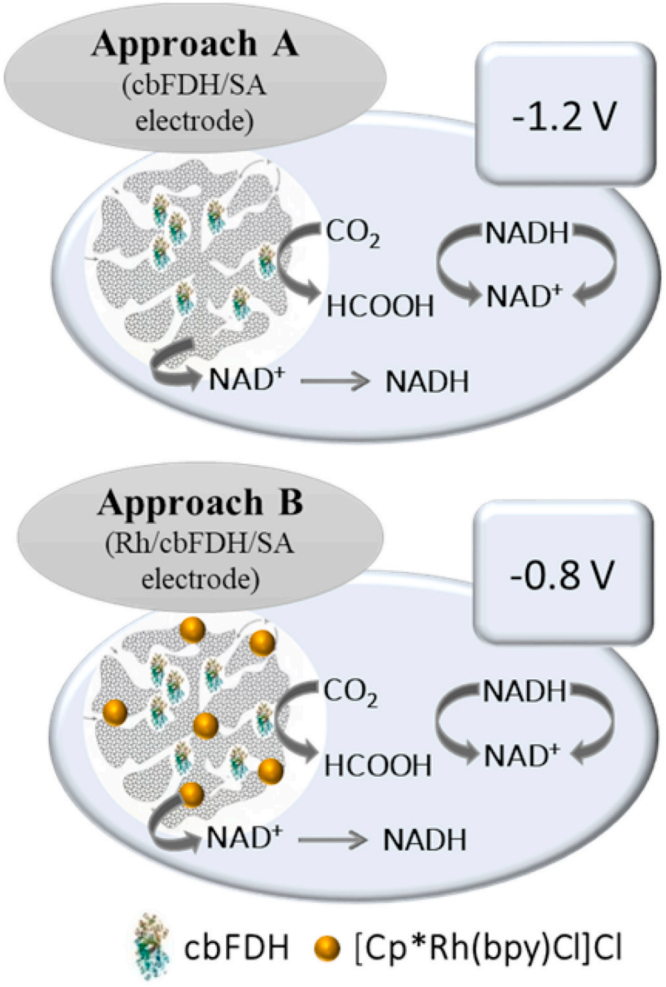

Fig. 4. Electrochemical approaches explored for the production of FA using the CbFDH/SA based electrodes in the absence (approach A) and presence (approach B) of the nanoconfined [Cp*Rh (bpy)Cl]Cl on the mesoporous carbon SA.

the beneficial effect of the nanoconfinement on the performance and efficiency of the biocathode. Other authors have studied the $BERCO_2$ using metallic-FDH (Hartmann and Leimkühler, 2013), as well as other cathodes (e.g., glassy carbon, graphite) (Srikanth et al., 2014, 2017) and redox mediators (Jayathilake et al., 2019), with still lower performance ($3.1{\cdot}10^{-3}$ μmol min^{-1} U^{-1}) (Choi et al., 2018) than that herein reported ($33.0{\cdot}10^{-3}$ μmol min^{-1} U^{-1}).

Regarding the coulombic efficiency, herein reported values are in line with those found in the literature for a similar applied potential of −0.8 V (e.g., 13% for CbFDH immobilized on graphite using neutral red as mediator (Choi et al., 2018; Zhang et al., 2016a); 68% for CbFDH immobilized in a Nafion modified micellic film on a graphitic electrode (Zhang et al., 2016b)). Nevertheless, these coulombic efficiencies are still far from those reported for the system CbFDH and carbonic hydrogenase (ca. 92%) (Srikanth et al., 2017) or other types of formate dehydrogenases (Reda et al., 2008; Bassegoda et al., 2014). Nevertheless, it should be considered that the coulombic efficiencies depend intrinsically of the type of the FDH enzyme (Bassegoda et al., 2014). More recently, Jayathilake et al. (2019) reported an outstanding current efficiency of over 96% recalculated after subtraction of the parasitic reactions in a three compartment electrochemical cell using methyl viologen as cofactor. Despite the high efficiency of their approach, the instability of the cofactor in the presence of molecular oxygen makes the process it unfeasible from a scaling point of view. Indeed, despite the

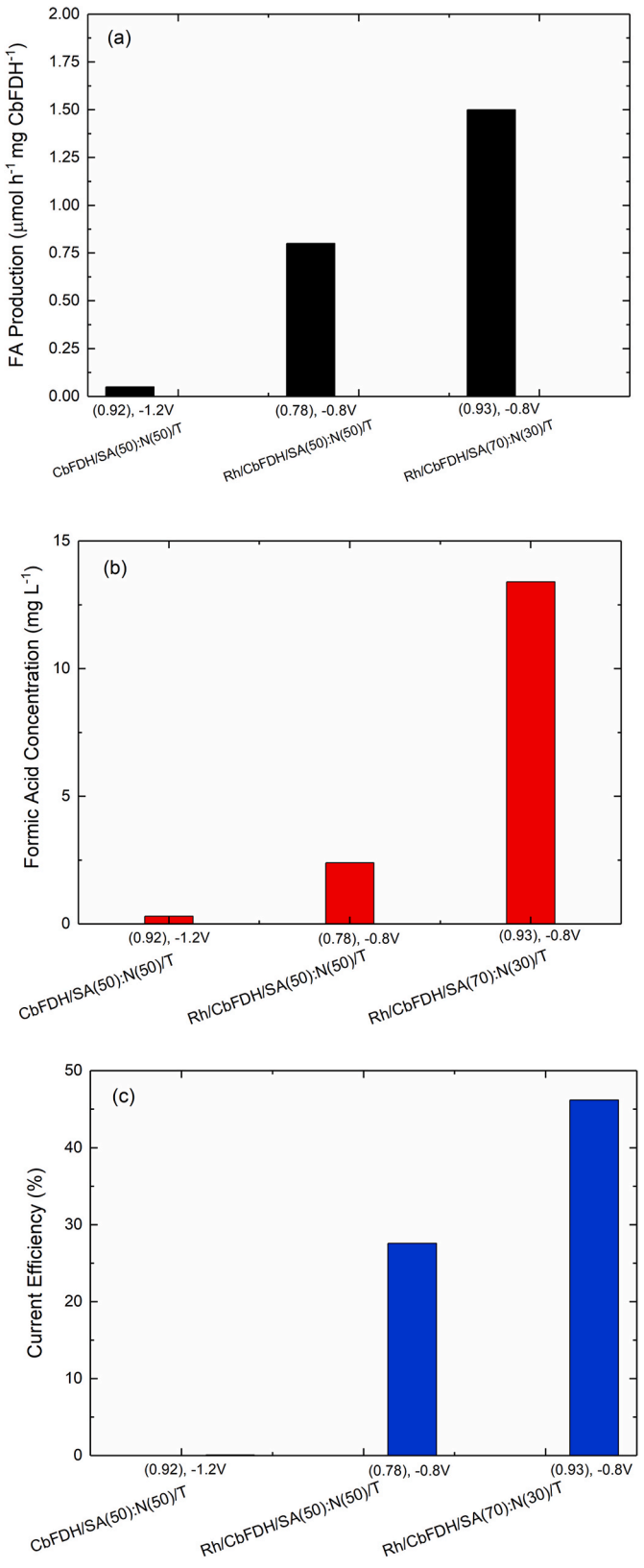

Fig. 5. FA production per hour and amount of immobilized enzyme (a), concentration (b) and current efficiencies (c) for FA production. Reaction time 5 h. Coverage Γ in mg cm^{-2} of each electrode is indicated between brackets; applied potential (−0.8 or −1.2V) is also indicated.

inherent disadvantages of NADH as cofactor for the bioelectroreduction of CO_2 using FDH, Chen et al. (2019) have reported a production rate of 13.2 μmol min^{-1} using NADH, a Rh complex and mesoporous NU-1006 MOF.

NAD-dependent CbFDH is very selective for the CO_2/formate couple, so it is very unlikely that the low coulombic efficiency is due to the enzyme denaturation or poor accessibility of NADH or CO_2 species. This behavior would be most likely attributed to the occurrence of competitive electrochemical processes, such as the electrocatalytic formation of hydrogen catalyzed by the Rh(I)–H complex (Taheria and Berben, 2016) or by the carbon support (Paul et al., 2019; Hu and Dai, 2016). Another aspect that needs to be highlighted is the adsorption of NADH on the carbon support during the evolution of the reaction (Banks and Compton, 2005), which can lead not only to a depletion of NADH in the solution but also to an inefficient NADH regeneration by the redox mediator, thereby yielding low Coulombic efficiency. The most plausible explanation for our results based on NADH dependent systems could be found on the following mechanism (Steckhan et al., 1991) occurring in the nanopore carbon:

$$[Cp*Rh(III)(bpy)Cl]^+ + e^- \rightarrow [Cp*Rh(II)(bpy)Cl] \quad (5)$$

$$[Cp*Rh(II)(bpy)Cl] + e^- \rightarrow [Cp*Rh(I)(bpy)] + Cl^- \quad (6)$$

$$[Cp*Rh(I)(bpy)] + H^+ \rightarrow [Cp*Rh(III)H(bpy)]^+ \quad (7)$$

Then, the catalytic NADH regeneration would proceed as follows:

$$[Cp*Rh(III)H(bpy)]^+ + Cl^- + NAD^+ \rightarrow [Cp*Rh(III)(bpy)Cl]^+ + NADH \quad (8)$$

Indeed, it has been demonstrated at the Rh complex [Cp*Rh(III)(bpy)Cl]$^+$ can promote the homogeneous catalytic reduction of the cofactor in the presence of a donor like formate (Ruppert et al., 1988), following reactions (9) and (10). This could contribute to the partial depletion of FA, thereby leading to a decrease in the production rate. The [Cp*Rh(III)H (bpy)Cl] species (reaction (10)) in the presence of NAD^+ would yield NADH and the regenerated form of the redox mediator.

$$[Cp*Rh(III)(bpy)Cl]^+ + \text{formate} \rightarrow [Cp*Rh(III)(bpy)\text{formate}]^+ + Cl^- \quad (9)$$

$$[Cp*Rh(III)(bpy)\text{formate}]^+ + Cl^- \rightarrow [Cp*Rh(III)H(bpy)Cl] + CO_2 \quad (10)$$

Even though reactions (9)–(10) occur in solution, we have to be critical with the role of the formate oxidation under the above Michaelis-like type reaction when the complex mediator is immobilized in the nanoporous carbon. The reverse reaction of formate oxidation may also occur in the presence of CbFDH enzyme immobilized in the nanoporous carbon, as the local concentration of FA in the pores (where the biomolecule is adsorbed) exceeds the solubility of CO_2; thereby reducing the activity yield of the enzyme towards FA production. This hypothesis would be supported by the studies of Barin et al. (2019) reporting a semi-continuous process for the separation of $BERCO_2$ to FA from the NADH/NAD + system using CbFDH immobilized in polystyrene nanofibers.

The contribution of the electrochemical reduction of CO_2 to FA formation upon the Rh (I) complex immobilized on the porous carbon support in the absence of the enzyme at our experimental conditions (i.e., −0.8 V vs Ag/AgCl) was confidently discarded based on the abundant studies from the literature reporting a negligible activity at potentials below -1V vs Ag/AgCl (Caix et al., 1997; Kim et al., 2014; Chen et al., 2019). As an example, Chen et al. (2019) reported no formate electrocatalytic production over a mesoporous MOF using NADH cofactor and the Rh complex (Cp*Rh (2,2′-bipyridyl-5,5′-dicarboxylic acid) at −1.1 V vs AgCl/Ag; on the other hand, Caix et al. (1997) explored the electrochemical reduction of CO_2 into FA (50%) and CO (<30%) using the same Rh complex [Cp*Rh (bpy)Cl]Cl at electrode potential of −1.64 V vs SCE (i.e., considerably higher than that used in this work). Accordingly, the only competitive process would be the formation of hydrogen catalyzed by the Rh(I)–H complex species and/or the carbon support (*vide supra)*.

In this work, we have used a nanoporous carbon of hydrophobic nature, which surface composition as measured by XPS is: 90.9 at.% of C, 9.08 at.% of O and <0.2 at.% of P (Fig. ESI-4) and displaying high affinity towards the adsorption of CO_2. This may lead to an oversolubility of CO_2 compared to the bulk, as well as to a lower hydration or formation of hydrogencarbonate ions under the nanoconfinement (Li et al., 2020), thereby reducing the reverse reaction (reaction (1)) and thus enhancing the coulombic efficiency of formate production.

Chronoamperometric experiments recorded at −0.8 V on the biocathodes Rh/CbFDH/SA(x):N(y)/T rendered a constant current density not higher than 0.08 mA cm^{-2} during the electrolysis, regardless the electrodes carbon loading coverage (the current density decreased with the increase in the Nafion content). This current density value is lower than that reported for other mFDH enzymes in solution (ca. 0.55 mA cm^{-2}) (Choi et al., 2018), which is expected since we are reporting the electrocatalytic activity in a nanoconfined state. Such behavior could be attributed to either accessibility restrictions of NAD^+ cofactor to reach the redox mediator, or to diffusional problems of CO_2 inside the tortuous pore network of the carbon support. Thus, further studies would be necessary to clarify the effect of the pore accessibility of CO_2 on the carbon support to prevent gas diffusion issues, compared to the tight pore confinement of the immobilized enzyme. Future research should also be conducted with different NADH concentration to showcase the NADH regeneration with respect to the immobilized [Cp*Rh (bpy)Cl]$^+$ with time-on-stream, to investigate other redox mediators as alternatives to the rhodium complex, and to explore their application in polymer electrolyte membrane electrochemical reactors (based on the excellent long-term stability of herein prepared biocathodes). Indeed, the regeneration and the reuse of the cofactor remain as the main challenges for a durable and robust large scale deployment in the market for the $BERCO_2$.

4. Conclusions

The co-immobilization of formate dehydrogenase from *Candida boidinii* (CbFDH) and the Rh complex mediator [Cp*Rh (bpy)Cl]Cl on a nanoporous carbon with a well-developed nanopore architecture has been investigated for the bioelectrochemical conversion of CO_2 into formic acid. The enzyme nanoconfined in the nanoporous carbon retained its enzymatic activity, and provided a higher FA production rate in the presence of NADH, compared to results obtained with the non-immobilized enzyme in solution. Furthermore, the co-immobilization of a rhodium redox mediator on the nanoporous carbon which is used for the regeneration of the cofactor was successfully performed, without hindering the enzymatic activity of CbFDH. The incorporation of Nafion as binder in the preparation of the biocathodes did not modify the immobilization rate or the performance of the enzyme, allowing the fabrication of relatively large electrodes (i.e., 2 cm × 3 cm). Despite a low amount of enzyme immobilized, the electrocatalytic activity of the biocathode by incorporating different Nafion to nanoporous carbon ratios was superior in terms of formic acid production rates than that of the enzyme in solution. Coulombic efficiencies ranged between 25 and 46%, with the highest value obtained for the biocathode prepared with the highest nanoporous carbon to Nafion ratio and the highest coverage. In addition to this, the biocathodes showed excellent long-term stability. These results are most promising for the bioelectrosynthesis of formic acid at large scale (beyond laboratory scale with small electrodes), and forecast interesting perspectives on the use of bioelectrochemical systems for the synthesis of chemicals and fuels centered on the immobilization of FDH on nanoporous carbons with

adequate pore structure, as well as their application in polymer electrolyte membrane electrochemical reactors.

Authors contributions statement

Naiara Hernández Ibáñez, Alicia Gomis and Jesus Iniesta performed the whole experimental work. All the authors participated in the discussion of results and writing of the whole manuscript.

Declaration of competing interest

The authors declare that they have no known competing financial interests or personal relationships that could have appeared to influence the work reported in this paper.

Acknowledgments

NH, VM and JI thank Spanish MINICINN (projects CTQ2016- 76231-C2-2-R and PID2019-108136RB-C32) for financial support. COA thanks the financial support of the European Research Council through a Consolidator Grant (PHOROSOL 684161).

Appendix A. Supplementary data

Supplementary data related to this article can be found at https://doi.org/10.1016/j.chemosphere.2021.133117.

References

Addo, P.K., Arechederra, R.L., Waheed, A., Shoemaker, J.D., Sly, W.S., Minteer, S.D., 2011. Methanol production via bioelectrocatalytic reduction of carbon dioxide: role of carbonic anhydrase in improving electrode performance. Electrochem. Solid State Lett. 14 (4), E9–E13.

Ali, I., Khan, T., Omanovic, S., 2014. Direct electrochemical regeneration of the cofactor NADH on bare Ti, Ni, Co and Cd electrodes: the influence of electrode potential and electrode material. J. Mol. Catal. Chem. 387, 86–91.

Alissandratos, A., Kim, H.K., Easton, C.J., 2013. Formate production through biocatalysis. Bioengineered 4 (5), 348–350.

Amao, Y., 2018. Formate dehydrogenase for CO2 utilization and its application. J. CO_2 Utilization 26, 623–641.

Appel, A.M., J Bercaw, E., Bocarsly, A.B., Dobbek, H., Dubois, D.L., Dupuis, M., Ferry, J. G., Fujita, E., Hille, R.P., Kenis, J.A., Kerfeld, C.A., Morris, R.H., Peden, C.H.F., Portis, A.R., Ragsdale Rauchfuss, S.W., Reek, T.B., Seefeldt, L.C., Thauer, R.K., Waldrop, G.L., 2013. Frontiers, opportunities, and challenges in biochemical and chemical catalysis of CO2 fixation. Chem. Rev. 113 (8), 6621–6658.

Azem, A., Man, F., Omanovic, S., 2004. Direct regeneration of NADH on a ruthenium modified glassy carbon electrode. J. Mol. Catal. Chem. 219 (2), 283–299.

Banks, C.E., Compton, R.G., 2005. Exploring the electrocatalytic sites of carbon nanotubes for NADH detection: an edge plane pyrolytic graphite electrode study. Analyst 130 (9), 1232–1239.

Barin, R., Biria, D., Rashid-Nadimi, S., Asadollahi, M.A., 2019. Investigating the enzymatic CO_2 reduction to formate with electrochemical NADH regeneration in batch and semi-continuous operations. Chem. Eng. & Processing-Process Intensification 140, 78–84.

Bassegoda, A., Madden, C., Wakerley, D.W., Reisner, E., Hirst, J., 2014. Reversible interconversion of CO_2 and formate by a molybdenum-containing formate dehydrogenase. J. Am. Chem. Soc. 136 (44), 15473–15476.

Bolivar, J.M., Wilson, L., Ferrarotti, S.A., Fernandez-Lafuente, R., Guisan, J.M., Mateo, C., 2007. Evaluation of different immobilization strategies to prepare an industrial biocatalyst of formate dehydrogenase from Candida boidinii. Enzym. Microb. Technol. 40 (4), 540–546.

Caix, C., Chardon-Noblat, S., Deronzier, A., 1997. Electrocatalytic reduction of CO_2 into formate with [(η5-Me5C5)M(L)Cl]+ complexes (L=2,2′-bipyridine ligands; M =Rh (III) and Ir(III)). J. Electroanal. Chem. 434, 163–170.

Chapman, J., Ismail, A., Dinu, C., 2018. Industrial applications of enzymes: recent advances. Techniques, & Outlooks, Catalysts 8 (6), 238.

Chen, Y., Li, P., Noh, H., Kung, C.W., Buru, C.T., Wang, X., Zhang, X., Farha, O.K., 2019. Stabilization of formate dehydrogenase in a metal eorganic framework for bioelectrocatalytic reduction of CO2. Angew. Chem. Int. Ed. 58, 7682–7686.

Choi, E.-G., Yeon, Y.J., Min, K., Kim, Y.H., 2018. Communication-CO2 reduction to formate: an electro-enzymatic approach using a formate dehydrogenase from rhodobacter capsulatus. J. Electrochem. Soc. 165 (9), H446–H448.

Cordas, C.M., Campanico, M., Baptista, R., Maia, L.B., Moura, I., Moura, J.J.G., 2019. Direct electrochemical reduction of carbon dioxide by a molybdenum-containing formate dehydrogenase. J. Inorg. Biochem. 196.

Cui, X., Li, C.M., Zang, J., Yu, S., 2007. Highly sensitive lactate biosensor by engineering chitosan/PVI-Os/CNT/LOD network nanocomposite. Biosens. Bioelectron. 22 (12), 3288–3292.

Del Castillo, A., Alvarez-Guerra, M., Solla-Gullón, J., Sáez, A., Montiel, V., Irabien, A., 2015. Electrocatalytic reduction of CO2 to formate using particulate Sn electrodes: effect of metal loading and particle size. Appl. Energy 157, 165–173.

Demir, A.S., Talpur, F.N., Sopaci, S.B., Kohring, G.W., Celik, A., 2011. Selective oxidation and reduction reactions with cofactor regeneration mediated by galactitol-, lactate-, and formate dehydrogenases immobilized on magnetic nanoparticles. J. Biotechnol. 152 (4), 176–183.

Diaz-Sainz, G., Alvarez-Guerra, M., Solla-Gullon, J., Garcia-Cruz, L., Montiel, A., Irabien, V., 2020. Gas-liquid-solid reaction system for CO(2)electroreduction to formate without using supporting electrolyte. AIChE J 66.

Finn, C., Schnittger, S., Yellowlees, L.J., Love, J.B., 2012. Molecular approaches to the electrochemical reduction of carbon dioxide. Chem. Commun. 48 (10), 1392–1399.

Hartmann, T., Leimkühler, S., 2013. The oxygen-tolerant and NAD+-dependent formate dehydrogenase from Rhodobacter capsulatus is able to catalyze the reduction of CO_2 to formate. FEBS J. 280 (23), 6083–6096.

Hernández, S., Farkhondehfal, M.A., Sastre, F., Makkee, M., Saracco, G., Russo, N., 2017. Syngas production from electrochemical reduction of CO2: current status and prospective implementation. Green Chem. 19 (10), 2326–2346.

Hernández-Ibáñez, N., Montiel, V., Gomis-Berenguer, A., Ania, C.O., Iniesta, J., 2021. Effect of confinement of horse heart cytochrome c and formate dehydrogenase from Candida boidinii on mesoporous carbons on their catalytic activity. Bioproc. Biosyst. Eng. 44, 1699–1710.

Hernández-Ibáñez, N., Montiel, V., Molina-Jorda, J.M., Iniesta, J., 2018. Fabrication, characterization and electrochemical response of pitch-derived open-pore carbon foams as electrodes. Bioprocess J. Appl. Electrochem. 48, 329–342.

Hollmann, F., Witholt, B., Schmid, A., 2002. [Cp*Rh(bpy)(H2O)]2+: a versatile tool for efficient and non-enzymatic regeneration of nicotinamide and flavin coenzymes. J. Mol. Catal. B Enzym. 19–20, 167–176.

Hu, C., Dai, L., 2016. Carbon-based metal-free catalysts for electrocatalysis beyond the ORR. Angew. Chem. Int. Ed. 55, 11736–11758.

Hu, C., Xiao, Y., Zou, Y., 2018. Carbon-based metal-free electrocatalysis for energy conversion, energy storage, and environmental protection. Electrochem. Energ. Rev. 1, 84–112.

Hwang, H., Yeon, Y.J., Lee, S., Choe, H., Jang, M.G., Cho, D.H., Park, S., Kim, Y.H., 2015. Electro-biocatalytic production of formate from carbon dioxide using an oxygen-stable whole cell biocatalyst. Bioresour. Technol. 185, 35–39.

Jayathilake, B.S., Bhattacharya, S., Vaidehi, N., Narayanan, S.R., 2019. Efficient and selective electrochemically driven enzyme-catalyzed reduction of carbon dioxide to formate using formate dehydrogenase and an artificial cofactor. Acc. Chem. Res. 52 (3), 676–685.

Jollie, D.R., Lipscomb, J.D., 1991. Formate dehydrogenase from methylosinus trichosporium Ob3b: purification and spectroscopic characterization of the cofactors. J. Biol. Chem. 266 (32), 21853–21863.

Kaneko, K., Rodríguez-Reinoso, F. (Eds.), 2019. Nanoporous Materials for Gas Storage. Springer Nature Singapore.

Kanth, B.K., Lee, J., Pack, S.P., 2013. Carbonic anhydrase: its biocatalytic mechanisms and functional properties for efficient CO2 capture process development. Eng. Life Sci. 13, 422–431.

Karaman, C., 2021. Boosting effect of nitrogen and phosphorous Co-doped three-dimensional graphene architecture: highly selective electrocatalysts for carbon dioxide electroreduction to formate. Top. Catal. 1, 1–10.

Kim, S., Koo, M., Sang, K., Lee, H., Yoon, S., Jung, K.-D., 2014. Conversion of CO2 to formate in an electroenzymatic cell using Candida boidinii formate dehydrogenase. J. Mol. Catal. B Enzym. 102, 9–15.

Lanjekar, K., Gharat, N., 2011. In Vitro Enzyme Catalytic Biotransformation of Carbon Dioxide into Useful Chemicals - A Short Review. International Conference on Green Technology and Environmental Conservation, GTEC-2011, Chennai, pp. 112–117.

Li, Q., Zhu, W., Fu, J., Zhang, H., Wu, G., Sun, S., 2016. Controlled assembly of Cu nanoparticles on pyridinic-N rich graphene for electrochemical reduction of CO_2 to ethylene. Nanomater. Energy 24, 1–9.

Li, W., Nan, Y., Zhang, Z., You, Q., 2020. Hydrophilicity/hydrophobicity driven CO_2 solubility in kaolinite nanopores in relation to carbon sequestration. Chem. Eng. J. 398, 125449.

Li, W., Seredych, M., Rodríguez-Castellón, E., Bandosz, T.J., 2016. Metal-free nanoporous carbon as a catalyst for electrochemical reduction of CO_2 to CO and CH_4. ChemSusChem 9, 606–616.

Liu, M., Pang, Y., Zhang, B., De Luna, P., Voznyy, O., Xu, J., Zheng, X., Dinh, C.T., Fan, F., Cao, C., de Arquer, F.P.G., Safaei, T.S., Mepham, A., Klinkova, A., Kumacheva, E., Filleter, T., Sinton, D., Kelley, S.O., Sargent, E.H., 2016. Enhanced electrocatalytic CO_2 reduction via field-induced reagent concentration. Nature 537, 382.

Lu, X., Tan, T.H., Ng, Y.H., Amal, R., 2016. Back cover: highly selective and stable reduction of CO2 to CO by a graphitic carbon nitride/carbon nanotube composite electrocatalyst. Chem. Eur J. 22 (34), 12200.

Lu, Y., Jiang, Z.-y., Xu, S.-W., Wu, H., 2006. Efficient conversion of CO_2 to formic acid by formate dehydrogenase immobilized in a novel alginate-silica hybrid gel, Catal. Today Off. 115 (1–4), 263–268.

Marinoiu, A., Carcadea, E., Cobzaru, C., Cernatescu, C., 2017. Numerical approach for catalytic conversion of CO_2 to methane over nickel base catalysts. Rev. Chim. (Bucharest) 68 (1), 128–133.

Moiroux, J., Elving, P.J., 1979. Adsorption phenomena in the NAD+/NADH system at glassy carbon electrodes. J. Electroanal. Chem. Interfacial Electrochem. 102, 93–108.

Nakata, K., Ozaki, T., Terashima, C., Fujishima, A., Einaga, Y., 2014. High-yield electrochemical production of formaldehyde from CO_2 and seawater. Angew. Chem. Int. Ed. 53 (3), 871–874.
Noji, T., Jin, T., Nango, M., Kamiya, N., Amao, Y., 2017. CO_2 photoreduction by formate dehydrogenase and a Ru-complex in a nanoporous glass reactor. ACS Appl. Mater. Interfaces 9 (4), 3260–3265.
Paul, J., Da, Q., Hu, C., Dai, L., 2019. Ten years of carbon-based metal-free electrocatalysts. Carbon Energy 1, 19–31.
Reda, T., Plugge, C.M., Abram, N.J., Hirst, J., 2008. Reversible interconversion of carbon dioxide and formate by an electroactive enzyme. Proc. Natl. Acad. Sci. U.S.A. 105 (31), 10654–10658.
Rees, N.V., Compton, R.G., 2011. Sustainable energy: a review of formic acid electrochemical fuel cells. J. Solid State Electrochem. 15 (10), 2095–2100.
Ren, S., Wang, Z., Bilal, M., Feng, M., Feng, Y., Jiang, Y., Jia, S., Cui, J., 2020. Co-immobilization multienzyme nanoreactor with co-factor regeneration for conversion of CO_2. Int. J. Biol. Macromol. 155, 110–118.
Rouf, S., Greish, Y.E., Al-Zuhair, S., 2021. Immobilization of formate dehydrogenase in metal organic frameworks for enhanced conversion of carbon dioxide to formate. Chemosphere 267, 128921.
Ruppert, R., Herrmann, S., Steckhan, E., 1988. Very Efficient reduction of NAD(P)+ with formate catalyzed by cationic rhodium complexes. J. Chem. Soc., Chem. Commun. 17, 1150–1151.
Sakai, K., Kitazumi, Y., Shirai, O., Kano, K., 2016a. Bioelectrocatalytic formate oxidation and carbon dioxide reduction at high current density and low overpotential with tungsten-containing formate dehydrogenase and mediators. Electrochem. Commun. 65, 31–34.
Sakai, K., Kitazumi, Y., Shirai, O., Takagi, K., Kano, K., 2016b. Efficient bioelectrocatalytic CO_2 reduction on gas-diffusion-type biocathode with tungsten-containing formate dehydrogenase. Electrochem. Commun. 73 (2016), 85–88.
Sakai, K., Kitazumi, Y., Shirai, O., Takagi, K., Kano, K., 2017a. Direct electron transfer-type four-way bioelectrocatalysis of CO_2/formate and NAD+/NADH redox couples by tungsten-containing formate dehydrogenase adsorbed on gold nanoparticle-embedded mesoporous carbon electrodes modified with 4-mercaptopyridine. Electrochem. Commun. 84, 75–79.
Sakai, K., Sugimoto, Y., Kitazumi, Y., Shirai, O., Takagi, K., Kano, K., 2017b. Direct electron transfer-type bioelectrocatalytic interconversion of carbon dioxide/formate and NAD(+)/NADH redox couples with tungsten-containing formate dehydrogenase. Electrochim. Acta 228, 537–544.
Sánchez-Sánchez, C.M., Expósito, E., Solla-Gullón, J., García-García, V., Montiel, V., Aldaz, A., 2003. Calculation of the characteristic performance indicators in an electrochemical process. J. Chem. Education 80, 529.
Schirwitz, K., Schmidt, A., Lamzin, V.S., 2007. High-resolution structures of formate dehydrogenase from Candida boidinii. Protein Sci. 16 (6), 1146–1156.
Schlager, S., Dumitru, L.M., Haberbauer, M., Fuchsbauer, A., Neugebauer, H., Hiemetsberger, D., Wagner, A., Portenkirchner, E., Sariciftci, N.S., 2016. Electrochemical reduction of carbon dioxide to methanol by direct injection of electrons into immobilized enzymes on a modified electrode. ChemSusChem 9 (6), 631–635.
Sivanesan, D., Yoon, S., 2013. Functionalized bipyridyl rhodium complex capable of electrode attachment for regeneration of NADH. Polyhedron 57, 52–56.
Sokol, K.P., Robinson, W.E., Oliveira, A.R., Warnan, J., Nowaczyk, M.M., Ruff, A., Pereira, I.A.C., Reisner, E., 2018. Photoreduction of CO_2 with a formate dehydrogenase driven by photosystem II using a semi-artificial Z-scheme Architecture. J. Am. Chem. Soc. 140 (48), 16418–16422.
Song, Y., Wang, S., Chen, W., Li, S., Feng, G., Wei, W., Sun, Y., 2020. Enhanced ethanol production from CO_2 electroreduction at micropores in nitrogen-doped mesoporous carbon. ChemSusChem 13, 293–297.
Srikanth, S., Maesen, M., Dominguez-Benetton, X., Vanbroekhoven, K., Pant, D., 2014. Enzymatic electrosynthesis of formate through CO_2 sequestration/reduction in a bioelectrochemical system (BES), Bioresour. Technol. 165, 350–354.
Srikanth, S., Alvarez-Gallego, Y., Vanbroekhoven, K., Pant, D., 2017. Enzymatic electrosynthesis of formic acid through carbon dioxide reduction in a bioelectrochemical system: effect of immobilization and carbonic anhydrase addition. ChemPhysChem 18 (22), 3174–3181.
Steckhan, E., Herrmann, S., Ruppert, R., Dietz, E., Frede, M., Spika, E., 1991. Analytical study of a series of substituted (2,2′-bipyridyl) (pentamethylcyclopentadienyl) rhodium and -iridium complexes with regard to their effectiveness as redox catalysts for the indirect electrochemical and chemical reduction of NAD(P)+. Organometallics 10 (5), 1568–1577.
Taheria, A., Berben, L.A., 2016. Making C–H bonds with CO_2: production of formate by molecular electrocatalysts. Chem. Commun. 52, 1768–1777.
Tan, B., Hickey, D.P., Milton, R.D., Giroud, F., Minteer, S.D., 2015. Regeneration of the NADH cofactor by a rhodium complex immobilized on multi-walled carbon nanotubes. J. Electrochem. Soc. 162 (3), H102–H107.
Walcarius, A., Nasraoui, R., Wang, Z., Qu, F., Urbanova, V., Etienne, M., Göllü, M., Demir, A.S., Gajdzik, J., Hempelmann, R., 2011. Factors affecting the electrochemical regeneration of NADH by (2,2'-bipyridyl) (pentamethylcyclopentadienyl)-rhodium complexes: impact on their immobilization onto electrode surfaces. Bioelectrochemistry 82, 46–54.
Weckbecker, A., Gröger, H., Hummel, W., 2010. Regeneration of nicotinamide coenzymes: principles and applications for the synthesis of chiral compounds. Adv. Biochem. Eng. Biotechnol. 195–242.
Wu, H., Tian, C., Song, X., Liu, C., Yang, D., Jiang, Z., 2013. Methods for the regeneration of nicotinamide coenzymes. Green Chem. 15 (7), 1773–1789.
Wu, T., Wu, L.H., Knight, J.A., 1986. Stability of NADPH: effect of various factors on the kinetics of degradation. J Clinical Chem 32, 314–319.
Yang, Z.Y., Moure, V.R., Dean, D.R., Seefeldt, L.C., 2012. Carbon dioxide reduction to methane and coupling with acetylene to form propylene catalyzed by remodeled nitrogenase. Proc. Natl. Acad. Sci. U.S.A. 109 (48), 19644–19648.
Yu, X., Pickup, P.G., 2008. Recent advances in direct formic acid fuel cells (DFAFC). J. Power Sources 182 (1), 124–132.
Yuan, J., Zhi, W.Y., Liu, L., Yang, M.P., Wang, H., Lu, J.X., 2018. Electrochemical reduction of CO_2 at metal-free N-functionalized graphene oxide electrodes. Electrochim. Acta 282, 694–701.
Zhang, L., Liu, J., Ong, S.F., Li, Y., 2016a. Specific and sustainable bioelectro-reduction of carbon dioxide to formate on a novel enzymatic cathode. Chemosphere 162, 228–234.
Zhang, Z., Chi, M., Veith, G.M., Zhang, P., Lutterman, D.A., Rosenthal, J., Overbury, S.H., Dai, S., Zhu, H., 2016b. Rational design of Bi nanoparticles for efficient electrochemical CO_2 reduction: the elucidation of size and surface condition effects. ACS Catal. 6 (9), 6255–6264.
Zhao, S., Jin, R., Jin, R., 2018. Opportunities and challenges in CO_2 reduction by gold- and silver-based electrocatalysts: from bulk metals to nanoparticles and atomically precise nanoclusters. ACS Energy Letters 3 (2), 452–462.
Zhu, Q., Ma, J., Kang, X., Sun, X., Hu, J., Yang, G., Han, B., 2016. Electrochemical reduction of CO_2 to CO using graphene oxide/carbon nanotube electrode in ionic liquid/acetonitrile system. Sci. China Chem. 59 (5), 551–556.
Zou, X., Liu, M., Wu, J., Ajayan, P.M., Li, J., Liu, B., Yakobson, B.I., 2017. How nitrogen-doped graphene quantum dots catalyze electroreduction of CO_2 to hydrocarbons and oxygenates. ACS Catal. 7, 6245–6250.